*Am. J. Hum. Genet. 49:1263–1279, 1991*

# Localization of an Ataxia-Telangiectasia Locus to a 3-cM Interval on Chromosome 11q23: Linkage Analysis of 111 Families by an International Consortium

T. Foroud,*,† S. Wei,† Y. Ziv,§ E. Sobel,* E. Lange,*,† A. Chao,† T. Goradia,* Y. Huo,† A. Tolun,‖ L. Chessa,** P. Charmley,†,‡ O. Sanal,†† N. Salman,# C. Julier,‡‡ P. Concannon,§§ C. McConville,‖‖ A. M. R. Taylor,‖‖ Y. Shiloh,§ K. Lange,* and R. A. Gatti†

Departments of *Biomathematics, †Pathology, and ‡Microbiology and Immunology, University of California School of Medicine, Los Angeles; §Department of Human Genetics, Tel Aviv University, Tel Aviv; ‖Department of Biology, Bogazici University, and #Department of Pediatrics, Istanbul University, Istanbul; **Department of Medical Genetics, University La Sapienza, Rome; ††Department of Pediatrics, Hacettepe University, Ankara; ‡‡Centre d'Etudes du Polymorphisme Humain, Paris; §§Department of Immunology, Virginia Mason Research Center, and University of Washington School of Medicine, Seattle; and ‖‖Department of Cancer Studies, Cancer Research Campaign Laboratories, University of Birmingham, Birmingham, England

## Summary

**Linkage of at least two complementation groups of ataxia-telangiectasia (AT) to the chromosomal region 11q23 is now well established. We provide here an 18-point map of the surrounding genomic region, derived from linkage analysis of 40 CEPH families. On the basis of this map, 111 AT families from Turkey, Israel, England, Italy, and the United States were analyzed, localizing the AT gene(s) to an 8-cM sex-averaged interval between the markers STMY and D11S132/NCAM. A new Monte Carlo method for computing approximate location scores estimates this location as being at least $10^8$ times more likely than the next most likely interval, with a support interval midway between STMY and D11S132 that is either 5.2 cM (sex-averaged and conservatively based on 3 lod scores from the maximum-location score) or 2.8 cM (male specific, based on a 2.72:1 interval-specific female-to-male distance ratio).**

## Introduction

Ataxia-telangiectasia (AT) is an autosomal recessive disorder that afflicts children early in life (Boder 1985). Recent reports have shown that the gene or genes responsible for AT complementation groups A (Gatti et al. 1988*a;* Sanal et al. 1990) and C (Ziv et al. 1991) localize to the chromosomal region 11q23. Together, these two complementation groups constitute as much as 85% of tested AT patients (Jaspers et al. 1985, 1988). In addition, the gene responsible for complementation group D has also been assigned to chromosome 11q (Ejima et al. 1990; Komatsu et al. 1990). Thus, it would appear that most, if not all, of the genes responsible for AT map to 11q23. It is unclear whether these complementation groups represent different loci or intragenic defects in a single locus.

Further localization of AT within the 11q23 region depends on both a better genetic map of the region and linkage analyses of more families. To address the first of these two needs, we constructed a multipoint map of 18 marker loci concentrated in the 11q22–23 region. This map is based both on linkage analyses of normal families provided as part of the CEPH (Centre d'Etude du Polymorphisme Humaine) consortium (Dausset 1986; Dausset et al. 1990) and on data from pulsed-field gel electrophoresis (PFGE) experiments. To facilitate merging our map with other maps of chromosome 11q (Leppert et al. 1987; Maslen et al. 1988; Budarf et al. 1989; Charmley et al. 1990*a,* 1991; Concannon et al. 1990; Julier et al. 1990; Lichter et al. 1990; Wei et al. 1990), a few loci outside the 11q22–23 region were included.

To provide more definitive mapping of AT itself, we pooled typing data on 111 AT pedigrees from various

Received February 25, 1991; final revision received July 29, 1991.

Address for correspondence and reprints: Richard A. Gatti, M.D., Department of Pathology, UCLA School of Medicine, Los Angeles, CA 90024.


0002-9297/91/4906-0013$02.00

laboratories. Because many of the pedigrees are highly inbred and lack key individuals in early generations, it was impossible to calculate location scores with more than two markers and AT simultaneously. This dilemma prompted us to apply a new Monte Carlo method for the approximate calculation of location scores with large numbers of markers. This new technique is described in the accompanying paper by Lange and Sobel (1991). These three steps—precise marker ordering, increasing the number of AT families, and application of the simulation method—have allowed us to conclusively map an AT locus to the 8-cM interval between the markers stromelysin (STMY) and D11S132 (L424), with a male-specific support interval of 2.8 cM midway between these two markers. This improvement over the results of Gatti et al. (1988*a*), McConville et al. (1990*a*, 1990*b*), and Sanal et al. (1990) argues in favor of the genetic homogeneity of AT.

## Material and Methods

### *DNA Markers*

To create a more comprehensive marker map of the 11q22–23 region, we ordered 18 loci by using the DNA polymorphisms described in table 1. All RFLPs were detected by Southern blotting (Gatti et al. 1984; Charmley et al. 1990*a*). For the sake of brevity, the "D11" designation for anonymous probes on chromosome 11 has been omitted throughout the present report. RFLP typing of the Israeli (Ziv et al. 1991) and British (McConville et al. 1990*a*, 1990*b*) AT families was completed in the collaborating laboratories (by Y.S. and A.M.E.T., respectively), by using probes provided by a single laboratory (R.A.G.'s). Allelic frequencies shown in table 1 were either taken from the original references cited or, in the case of S147, derived from our own testing of CEPH parents. For some loci, haplotypes were created by using more than one probe/enzyme combination to phenotype the CEPH families, while the AT families were typed with only one marker from each haplotype, as indicated by the footnotes in table 1.

cDNA for the genes CD20 and stromelysin (STMY) was provided by T. Tedder (Tedder et al. 1988) and N. Spurr (Spurr et al. 1988), respectively. Both the cDNA clone pM1.3 from the mouse neural cell adhesion molecule (NCAM) gene (Goridis et al. 1985) and the human muscle NCAM cDNA clone NCAM3 (Dickson et al. 1987) were used to detect the human NCAM gene. cDNA for nearly the entire human tryosinase gene (TYR) was provided by M. Smith (Kwon et al. 1987). A human genomic lambda-phage clone from the 3′ portion of the human dopamine D2 receptor (DRD2) gene was provided by O. Civelli (Grandy et al. 1989). Cloned DNA segments from the apolipoprotein AI-CIII-AIV gene cluster (probes "I"–"X") were provided by S. Karathanasis (Mietus-Snyder et al. 1990). cDNA for CD3-epsilon (CD3E) and CD3-gamma (CD3G) was obtained from C. Terhorst (Gold et al. 1986; Krissansen et al. 1986), and the CD3-delta (CD3D) gene (van den Elsen et al. 1984) was purchased from the American Type Culture Collection (ATCC; Rockville, MD). A genomic clone containing the porphobilinogen deaminase (PBGD) gene was provided through M. Goossens (Llewellyn et al. 1987). DNA primers from the human thy-1 gene was used to amplify exon III from human genomic DNA by PCR, after which the unpurified DNA product was used to detect the thy-1 polymorphism. Different genomic sequences surrounding the *ets-1* gene were obtained from J. P. Kerckaert (Kerckaert et al. 1987), N. Sacchi (Sacchi et al. 1986), and the ATCC. Sources of probes for arbitrary sequences were as follows: p2-7-1D6 (S84) and p2-25 (S83) were obtained from M. Litt (Maslen et al. 1988); CJ52.208M2 (S351) and CJ52.75M1 (S385) were obtained from C. Julier (Julier et al. 1990); CRI-L424 (S132), CRI-L451 (S133), and CRI-R548 (S138) were purchased from Collaborative Research, Inc., (Bedford, MA); S144 (formerly called "pYNB3.12" or "MCT128.1") and HBI18P1 (S147) were obtained from Y. Nakamura (Carlson et al. 1988; Julier et al. 1989); and L7 (S29) was obtained from A. E. Retief (Warnich et al. 1986).

The following DNA polymorphisms used to construct our genetic map have been described elsewhere: CD20/*Msp*I (Charmley et al. 1990*b*); TYR/*Taq*I (Spritz et al. 1988); S84/*Taq*I (Maslen et al. 1988); S385/*Msp*I (Julier et al. 1990); STMY/*Taq*I (Spurr et al. 1988); S132/*Eco*RI and S132/*Hin*dIII (Donis-Keller et al. 1987); DRD2/*Taq*I (Grandy et al. 1989); CJ52.208M2(S351)/*Msp*I(1) and CJ52.208M2 (S351)/*Msp*I(2) (Julier et al. 1990); S144/*Msp*I (Carlson et al. 1988); APO "I–X" with *Pst*I, *Xba*I, *Xmn*I, *Msp*I, *Bgl*II, *Sca*I, and *Pvu*II (Mietus-Snyder et al. 1990); S29/*Taq*I (Warnich et al. 1986); CD3G/*Msp*I (Charmley et al. 1989*b*); CD3D/*Msp*I (Malhotra and Concannon 1989); CD3E/*Taq*I (Charmley et al. 1989*a*); PBGD/*Msp*I (Llewellyn et al. 1987); THY1/*Msp*I (Gatti et al. 1987, 1988*b*); S147/*Msp*I (Julier et al. 1989); S133/*Eco*RI and S133/*Msp*I (Charmley et

al. 1990*a*); S138/*Pst*I and S138/*Eco*RI (Charmley et al. 1990*a*); ETS1/*Sac*I and ETS1/*Xba*I (Sacchi et al. 1986; Kerckaert et al. 1987; Concannon et al. 1990); and S83/*Msp*I (Maslen et al. 1988).

### PFGE

PFGE studies were performed in a single laboratory (by R.A.G.) using a CHEF-DRII (contour-clamped homogeneous electric field) gel apparatus (BioRad, Richmond, CA). DNA from four or more individuals was isolated, in agarose, from lymphoblastoid cell lines, was digested, and was electrophoresed in 1% agarose gels with 0.5 × TBE buffer. Gels were typically run at a ramped pulse of 20–50 s at 200 V for 24 h at 14°C. Transfer of DNA to nylon membranes and subsequent hybridization with radiolabeled probes were performed essentially according to methods described elsewhere (Gatti et al. 1984; Reed and Mann 1985). Sizes of fragments were determined by comparison with standards consisting of *Saccharomyces cerevisiae* chromosomes.

### Pedigrees

An 18-point marker map of the 11q22–23 region was created by phenotyping either the original 40 CEPH consortium families or the expanded set of 61 CEPH families. The CEPH families are large nuclear families, with either or both sets of grandparents usually included. All CEPH families have a minimum of six offspring in the youngest generation. The original 40 families include over 500 individuals and potentially represent up to 750 informative meioses per locus (Dausset 1986; Dausset et al. 1990).

The 111 AT families included in the AT consortium data set are much more ethnically diverse than the CEPH families. Some collaborators concentrated on a few large highly inbred pedigrees with many affecteds (Gatti et al. 1988*a*; Sanal et al. 1990; Ziv et al. 1991), while others collected large numbers of small nuclear families (McConville et al. 1990*a*, 1990*b*). In all cases, the diagnosis of AT was established by clinicians with extensive experience and was based on the presence of (1) progressive cerebellar ataxia with onset in early childhood, (2) ocular apraxia, (3) nonrandom chromosomal aberrations, (4) elevated alpha-fetoprotein, (5) immunodeficiency, (6) family history, (7) telangiectasia and/or (8) abnormal in vitro response of fibroblast cultures to ionizing radiation (i.e., radioresistant DNA synthesis, as described by Young and Painter [1989]). Families with questionable diagnoses were excluded. The DNA of each family was prescreened for paternity by using Southern blots hybridized with the highly polymorphic D2S44 probe (Nakamura et al. 1987). Most families were not typed for complementation group. The international scope of this collaboration provided much greater ethnic and racial diversity than has any previous genetic analysis of AT. These families are further described in table 2. The diagnosis in American family ATV20 (table 2) is $AT_{Fresno}$ (Curry et al. 1989).

### Statistical Analysis

*A. CEPH data set.*—Prior to computation of lod scores, the CEPH genotypic data were simplified by the methods of Lange and Goradia (1987) and Lange and Weeks (1989). These simplifications improved computational efficiency without changing numerical results. All linkage calculations were performed using a new version of the computer program MENDEL (Lange et al. 1988). This version is specifically designed for multilocus mapping problems with large numbers of markers.

Our first priority was to order all 18 loci in one comprehensive map. An exhaustive consideration of all $3.2 \times 10^{15}$ (18!/2) orders would have been prohibitive. Fortunately, a somatic cell hybrid breakpoint located between S144 and APO (Wei et al. 1990) allowed us to divide the markers into two disjoint groups of nine markers each; each group was then ordered separately. Within each of these two marker groups, several loci had been previously ordered (Maslen et al. 1988; Charmley et al. 1990*a*, 1991; Julier et al. 1990). We merged and expanded these previous maps through a combination of pairwise lod scores and multipoint lod scores. With the exception of two unresolved pairs of loci (see below), a "best-supported order" with highest maximum lod score was attained in both halves of the map. Our strategy for ordering loci has been described in detail by Weeks and Lange (1987). A key element of this strategy is to test the stability of any proposed best order by inverting each subblock of loci within the order and then recomputing maximum lod scores.

The nine loci telomeric to S144 were especially favorable for ordering because a second somatic cell hybrid breakpoint telomeric to CD3 isolated the markers APO, S29, and CD3 (Wei et al. 1990) from the markers PBGD, THY1, S133, S147, ETS1, and S83. This physical finding reduced the number of possible orders and permitted a more definitive multipoint analysis of the nine loci telomeric to S144.

Through the creation of two distinct, nonoverlap-

**Table 1**

**Probe/Enzyme Polymorphisms**

| Locus (probe) | Family Group(s) Used | Enzyme | Allele Size(s) (kb) | Allele Frequency | Observed Heterozygosity | No. of AT Families Typed |
|---|---|---|---|---|---|---|
| CD20 (pB1-21A-29) | AT + CEPH | *Msp*I | 9.0 | .43 | .31 | 22 |
| | | | 6.0 | .57 | | |
| TYR (pmel34) | AT + CEPH | *Taq*I | 2.8 | .42 | .58 | 100 |
| | | | 2.7 and 2.4 | .42 | | |
| | | | 2.4 | .16 | | |
| D11S84 (p2-7-1D6) | AT + CEPH | *Taq*I | 6.4 | .24 | .40 | 106 |
| | | | 4.3 | .76 | | |
| D11S385 (CJ52.75M1) | AT + CEPH | *Msp*I | 5.5 | .87 | .17 | 108 |
| | | | 3.5 and 2.0 | .13 | | |
| STMY (psp64) | AT + CEPH | *Taq*I | 4.6 | .54 | .46 | 110 |
| | | | 2.1 and 1.0 | .46 | | |
| D11S132 (CRI-L424) | CEPH | Haplotype[a] | | .58 | .58 | |
| | | | | .30 | | |
| | | | | .06 | | |
| | | | | .06 | | |
| | AT | *Eco*RI | 8.0 | .62 | .55 | 110 |
| | | | 7.3 | .38 | | |
| DRD2 (HD2G1) | AT + CEPH | *Taq*I | 6.6 | .11 | .24 | 109 |
| | | | 3.7 and 2.9 | .89 | | |
| D11S351 (CJ52.208) | CEPH | Haplotype[b] | | .58 | .52 | |
| | | | | .36 | | |
| | | | | .05 | | |
| | AT | *Msp*I | 4.0 | .41 | .53 | 108 |
| | | | 3.2 | .59 | | |
| D11S144 (MCT128.1) | AT + CEPH | *Msp*I | 2.9 | .53 | .56 | 108 |
| | | | 2.6 | .47 | | |
| APO (apolipoprotein) | CEPH | Haplotype[c] | | .55 | .82 | |
| | | | | .28 | | |
| | AT | | | .17 | | |
| | | *Msp*I | 1.7 | .96 | .08 | 44 |
| | | | 1.0 | .04 | | |
| D11S29 (L7) | AT + CEPH | *Taq*I | 10.9 | .79 | .30 | 59 |
| | | | 13.9 | .21 | | |
| CD3 G/D/E | CEPH | Haplotype[d] | | .62 | .54 | |
| | | | | .29 | | |
| | | | | .08 | | |

(*continued*)

ping maps—one centromeric to S144 and the other telomeric to S144—we were able to reduce the computational load and increase efficiency. After concatenating the two "best-supported orders," we calculated one overlapping, combined 18-point map from CD20 to S83. Adjacent loci were then inverted to determine odds favoring the statistical stability of this proposed order.

*B. AT data set.*—The complex inbreeding loops and missing ancestors in the AT consortium pedigrees presented a computational challenge. As a first step in analysis, we computed pairwise lod scores between AT and all 18 markers. After pairwise lod score calculations, we performed traditional three-point location scores by using adjacent pairs of markers and AT, placing AT in the three possible positions relative to the two marker loci. The distance between markers was obtained from the 18-point map described above.

These calculations were followed by approximate computation of location scores, using the Monte Carlo simulation technique described in the accompanying paper by Lange and Sobel (1991). This tech-

**Table 1 (continued)**

| Locus (probe) | Family Group(s) | Enzyme | Allele Size(s) (kb) | Allele Frequency | Observed Heterozygosity | No. of AT Families Typed |
|---|---|---|---|---|---|---|
| CD3G (pT3dH)..... | AT | *Msp*I | 2.5 | .80 | .23 | 64 |
| | | | 1.7 and 0.8 | .20 | | |
| CD3D (pPBGC9)..... | AT | *Msp*I | 5.4 | .06 | .04 | 52 |
| | | | 4.6 | .94 | | |
| CD3E (pDJ4)..... | AT | *Taq*I | 8.7 | .67 | .41 | 58 |
| | | | 8.1 | .33 | | |
| PBGD (pUSE109)..... | AT + CEPH | *Msp*I | 3.0 | .43 | .52 | 57 |
| | | | 2.2 | .57 | | |
| THY1 (pCR502-505)..... | AT + CEPH | *Msp*I | 0.9 | .28 | .45 | 97 |
| | | | 0.8 | .72 | | |
| D11S147 (HBI18P1)..... | AT + CEPH | *Msp*I | 5.2 | .43 | .48 | 34 |
| | | | 4.8 | .57 | | |
| D11S133/D11S138 (CRI-L451/CRI-R548)... | CEPH | Haplotype[e] | | .70 | .53 | |
| | | | | .20 | | |
| | | | | .05 | | |
| | | | | .05 | | |
| | AT | *Eco*RI | 12.0 | .08 | .36 | 34 |
| | | | 10.8 | .92 | | |
| ETS1..... | CEPH | Haplotype[f] | | .62 | .57 | |
| | | | | .36 | | |
| | | | | .02 | | |
| | AT | *Xba*I | 2.4 | .09 | .17 | 35 |
| | | | 1.5 | .91 | | |
| D11S83 ..... | AT + CEPH | *Msp*I | 4.3 | .22 | .49 | 39 |
| | | | 3.2 and 1.1 | .78 | | |

[a] Consists of *Eco*RI and *Hin*dIII RFLP (Charmley et al. 1990*a*).
[b] Consists of *Msp*I(1) and *Msp*I(2) RFLP (Julier et al. 1990).
[c] Consists of seven probes and 10 enzymes (Mietus-Snyder et al. 1990).
[d] Consists of three probes and two enzymes (Charmley et al. 1989*a*, 1989*b*; Malhotra and Concannon 1989).
[e] Consists of two probes and three enzymes (Charmley et al. 1990*a*).
[f] Consists of two probes and one enzyme (Concannon et al. 1990; Charmley et al. 1991).

nique can analyze many markers, but all markers must be biallelic. Thus, we employed only 14 markers in this final location score computation.

## Results

### 1. *The Multipoint CEPH Map*

Table 3 displays maximum lod scores and corresponding recombination fraction estimates for each pair of loci between CD20 and S83, a sex-averaged distance of approximately 92 cM encompassing most of the long arm of chromosome 11. The maximum lod scores reflect the number of individuals typed, as well as the informativeness of each marker. Allelic frequencies are given in table 1. As can be seen in table 3*A*, two pairs of loci (STMY/S385 and S351/S144) showed no recombination (also see fig. 1). A unique "best-supported order" could not be established because the multipoint lod scores also estimate zero recombination between these pairs when the loci in each pair are adjacent. By fixing an arbitrary orientation of the two loci in each of these zero-recombination pairs, a single best order could be identified.

The two tightly linked pairs of loci were further analyzed by PFGE using "rare cutter" restriction enzymes. By serial probing of the same blot after complete "stripping" of the previous probe (Gatti et al. 1984) and by visual comparison of overlapping autoradiograms, we observed that STMY and S385 hybridized to DNA fragments of identical position when

## Table 2

**Families Included in AT Consortium Data Base**

| Family ID | No. of Individuals |
|---|---|
| United States: | |
| AT001 | 6 |
| AT002 | 4 |
| AT004 | 7 |
| AT006 | 9 |
| AT007 | 6 |
| AT009 | 5 |
| AT010 | 4 |
| AT011 | 11 |
| AT012 | 55[a] |
| AT014 | 5 |
| AT017 | 13[a] |
| AT018 | 6 |
| AT019 | 4 |
| ATV20 | 7 |
| AT021 | 9 |
| AT022 | 8 |
| AT023 | 7 |
| AT024 | 6 |
| KAT01 | 1[a] |
| Turkey (Ankara): | |
| TAT01 | 7 |
| TAT02 | 7[a] |
| TAT03 | 20[a] |
| TAT04 | 7[a] |
| TAT08 | 8[a] |
| TAT10 | 9 |
| TAT13 | 8[a] |
| TAT14 | 7[a] |
| TAT15 | 9[a] |
| TAT16 | 4[a] |
| TAT17 | 4[a] |
| TAT18 | 5[a] |
| TAT19 | 8[a] |
| TAT20 | 9[a] |
| TAT21 | 10[a,b] |
| TAT22 | 7[a,b] |
| TAT23 | 7[a,b] |
| TAT24 | 5[a,b] |
| TAT25 | 8[a,b] |
| TAT26 | 7[a,b] |
| TAT27 | 7[a,b] |
| TAT28 | 4[b] |
| Turkey (Istanbul): | |
| TIAT01 | 7[b] |
| TIAT03 | 8[a,b] |
| TIAT04 | 7[b] |
| TIAT05 | 6[b] |
| TIAT06 | 9[a,b] |
| TIAT07 | 7[a,b] |
| TIAT11 | 9[b] |
| TIAT12 | 7[a,b] |
| TIAT13 | 7[b] |
| TIAT15 | 4[b] |

(*continued*)

## Table 2 (continued)

| Family ID | No. of Individuals |
|---|---|
| Israel: | |
| ISAT01 | 49[a] |
| ISAT02 | 17[a] |
| ISAT03 | 17[a] |
| ISAT04 | 5 |
| ISAT05 | 11[a] |
| ISAT06 | 6 |
| ISAT07 | 6 |
| ISAT08 | 11[a] |
| ISAT09 | 30[a] |
| Italy: | |
| IAT01 | 2 |
| IAT02 | 4 |
| IAT05 | 4 |
| IAT06 | 3 |
| IAT07 | 5 |
| IAT09 | 5 |
| IAT11 | 17[a] |
| IAT12 | 6 |
| England: | |
| BR01 | 4 |
| BR02 | 4 |
| BR03 | 6 |
| BR04 | 4 |
| BR05 | 6 |
| BR06 | 5 |
| BR07 | 4 |
| BR08 | 4 |
| BR09 | 4 |
| BR10 | 5 |
| BR11 | 5 |
| BR12 | 5 |
| BR13 | 4 |
| BR14 | 4 |
| BR15 | 4 |
| BR16 | 4 |
| BR17 | 6 |
| BR18 | 4 |
| BR19 | 4 |
| BR20 | 4 |
| BR21 | 5 |
| BR22 | 6 |
| BR23 | 4 |
| BR24 | 5 |
| BR25 | 6 |
| BR26 | 5 |
| BR27 | 5 |
| BR28 | 4 |
| BR29 | 5 |
| BR30 | 4 |
| BR31 | 5 |
| BR32 | 5 |
| BR33 | 5 |
| BR34 | 4 |

(*continued*)

**Table 2 (continued)**

| Family ID | No. of Individuals |
|---|---|
| BR36 | 4 |
| BR37 | 5 |
| BR38 | 4 |
| BR39 | 4 |
| BR40 | 4 |
| BR41 | 4 |
| BR42 | 5 |
| BR45 | 4 |
| BR46 | 4 |

[a] Consanguineous family.

[b] Family omitted from Monte Carlo simulations, because of missing data or complicated pedigree structure.

the DNA was digested with *Sfi*I, *Cla*I, *Bss*HII, or *Xho*I; the smallest common fragment was approximately 60 kb (table 4). S144 and S351 also hybridized to fragments of identical positions, when the enzymes *Sfi*I, *Cla*I, and *Bss*HII were used; the smallest common fragment was approximately 150 kb (table 4). DNA fragments of identical positions were also noted with probes S132 and NCAM when two enzymes were used; the smallest common fragment was 340 kb (table 4). The fact that *Xho*I digests produced different-sized fragments with S132 and NCAM indicates that the two probes are not identical.

On the basis of hybridization to DNA from hybrid cell lines with X;11 and 4;11 translocations (Wei et al. 1990), we localized APO, S29, and CD3 between S144 and THY1. In addition, the loci PBGD, THY1, S147, S133, ETS1, and S83 all localized telomeric to the t4;11 breakpoint. Pairwise lod scores for all nine telomeric loci are displayed in table 3B. The three loci APO, S29, and CD3 were ordered by three-point maximum lod scores. The best order, APO–S29–CD3, placed S29 in the middle. The orientation centromere–APO–S29–CD3 is suggested by the partial map, centromere–S144–S29–CD3, of Charmley et al. (1990*a*). Of the six loci telomeric to the t4;11 breakpoint (PBGD, THY1, S147, S133, ETS1, and S83), only two—PBGD and S147—still required ordering (Charmley et al. 1990*a*; Concannon et al.

**Table 3**

**Maximum Lod Scores (below diagonal) and Maximum Likelihood Estimates of Recombination Fractions (above diagonal)**

A. Between Pairs of Nine Loci *Centromeric* to X;11 Translocation Breakpoint

| | CD20 | TYR | S84 | S385 | STMY | S132 | DRD2 | S351 | S144 |
|---|---|---|---|---|---|---|---|---|---|
| CD20 | | .11 | .26 | .39 | .31 | .16 | .18 | .34 | .20 |
| TYR | 7.38 | | .05 | .10 | .20 | .16 | .26 | .22 | .26 |
| S84 | .96 | 8.11 | | .03 | .12 | .17 | .13 | .14 | .18 |
| S385 | .01 | 2.62 | 5.57 | | .00 | .06 | .24 | .21 | .13 |
| STMY | .45 | 4.25 | 7.24 | 17.78 | | .09 | .21 | .18 | .16 |
| S132[a] | 2.90 | 4.12 | 7.37 | 8.27 | 16.69 | | .07 | .07 | .09 |
| DRD2 | 1.08 | .40 | 5.05 | 1.31 | 1.37 | 4.67 | | .09 | .11 |
| S351[a] | .44 | 3.87 | 7.23 | 2.34 | 5.92 | 21.61 | 8.03 | | .00 |
| S144 | 3.46 | 2.94 | 7.02 | 4.42 | 5.58 | 13.25 | 4.40 | 55.76 | |

B. Between Pairs of Nine Loci *Telomeric* to X;11 Translocation Breakpoint

| | APO | S29 | CD3 | PBGD | THY1 | S147 | S133 | ETS1 | S83 |
|---|---|---|---|---|---|---|---|---|---|
| APO[a] | | .05 | .05 | .04 | .06 | .07 | .16 | .20 | .25 |
| S29 | 24.71 | | .04 | .00 | .05 | .02 | .16 | .19 | .23 |
| CD3[a] | 42.36 | 19.21 | | .00 | .03 | .07 | .12 | .17 | .20 |
| PBGD | 35.08 | 12.94 | 21.98 | | .00 | .01 | .07 | .10 | .14 |
| THY1 | 30.24 | 15.30 | 27.05 | 15.35 | | .05 | .00 | .18 | .23 |
| S147 | 27.24 | 10.82 | 16.19 | 20.91 | 11.86 | | .06 | .13 | .50 |
| S133[a] | 5.45 | 1.44 | 2.85 | 9.19 | 3.53 | 5.47 | | .02 | .07 |
| ETS1[a] | 11.22 | 2.19 | 6.73 | 12.46 | 4.34 | 8.64 | 9.60 | | .10 |
| S83 | 3.05 | 1.01 | 4.45 | 5.85 | 2.37 | .00 | 4.09 | 7.35 | |

[a] Haplotype (see table 1 footnotes).

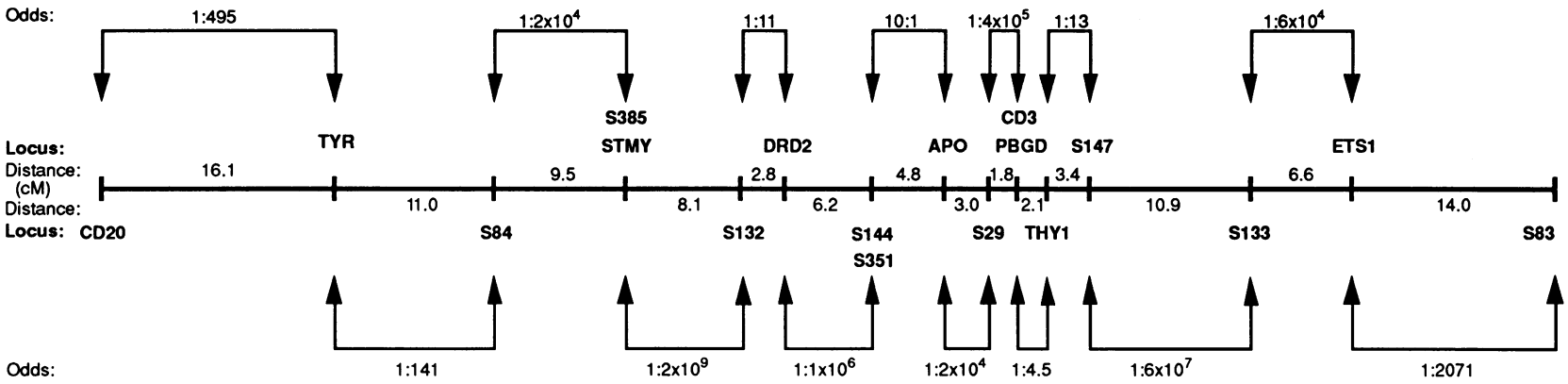


**Figure 1** Eighteen-point map of region surrounding AT gene at 11q23. Odds against inverting adjacent pairs of loci are given above or below the brackets. Distances between loci are based on sex-averaged recombination fractions.

**Table 4**

**Summary of PFGE Experiments**

| Probe | Approximate Fragment Size[a] (in kb) for Enzyme | | | |
|---|---|---|---|---|
| | *Sfi*I | *Cla*I | *Bss*HII | *Xho*I |
| STMY | 420 | 650 | 700 | 60 |
| | 340 | 600 | | |
| | 280 | 450 | | |
| | 220 | 410 | | |
| | 200 | 350 | | |
| | | 300 | | |
| | | 260 | | |
| | | 200 | | |
| | | 75 | | |
| | | 50 | | |
| S385 | 420 | 200 | 700 | 60 |
| | 340 | 75 | | |
| | 200 | | | |
| S132 | 440 | 445 | 370 | 80 |
| | 400 | | | 25 |
| | 380 | | | |
| | 340 | | | |
| NCAM | 440 | | 370 | 180 |
| | 400 | | | 75 |
| | 380 | | | |
| | 340 | | | |
| DRD2 | 80 | 290 | 200 | 90 |
| | | 240 | | |
| S351 | 150 | 415 | 650 | |
| | 100 | 340 | 380 | |
| | | 305 | 345 | |
| | | 265 | | |
| | | 245 | | |
| S144 | 150 | 340 | 380 | |
| | 30 | 265 | 345 | |
| | | 245 | | |

[a] The smallest fragments are assumed to represent complete digestion products. Additional cohybridizing bands were assumed to represent partial digestion products, allowing us to visualize some larger common fragments as well. Each fragment was observed in DNA from four or more individuals.

1990). Three-point maximum lod scores involving the triplets S29/PBGD/THY1 and THY1/S147/S133 effectively ordered the two new loci, PBGD and S147. Our final proposed order for the nine loci telomeric to S144 is shown in figure 1.

Five of the nine loci centromeric to the X;11 translocation had been previously ordered (Charmley et al. 1990*a*). Two of the three remaining loci—S385 and S351—are closely linked to STMY and S144, respectively. Examination of multipoint lod scores suggested the order shown in figure 1. This order was checked by first inverting blocks of loci within it and then looking for a higher maximum lod score. No such inversions led to a better order.

Merging the two maps on either side of S144 produced a combined map of 18 markers (fig. 1). To estimate distances between the 18 adjacent markers, we used a new version of MENDEL (Lange et al. 1988). No observed phenotypes or individuals were omitted from the analysis. Our success in this large-scale computation arose both from the incorporation of new algorithms in MENDEL and from the large memory and computational efficiency of an IBM 3090, on which the 18-point analysis was performed.

As a final check of the proposed order of figure 1, we inverted adjacent pairs of loci and recomputed maximum lod scores. These six-point lod scores always included the two closest flanking markers on either side of the pair of markers inverted. The odds against these inversions are also shown in figure 1. The only anomaly in these odds is the 10:1 odds favoring the alternative order centromere–APO–S144/S351, and this alternative was ruled out by the translocation data (Wei et al. 1990).

### 2. *Location Scores for AT*

The AT consortium data base offered a unique opportunity to further localize the AT gene or genes. The 111 families contained over 1,000 meioses. We first computed pairwise lod scores between AT and all marker loci. The resulting lod scores, summed over all AT families, are presented in table 5, along with the maximum lod scores, corresponding recombination fraction estimates, and their standard errors. As indicated, not all markers were completely typed in all families.

The results in table 5 confirm previously published reports indicating that AT is most likely located within the 17-cM sex-averaged interval from STMY to S144 (McConville et al. 1990*b*; Sanal et al. 1990). The highest lod scores with AT were found with the loci STMY, S351, S144, and S132. The four markers STMY, S132, DRD2, and S351 had estimated distances from AT that were less than 12 cM. Seven markers outside the interval from STMY to S144 gave maximum lod scores over 3.0; six had estimated distances from AT that were greater than 12 cM. This result would seem to dispel any conjecture that another AT gene may lie in the region of THY1 (Gatti et al. 1988*b*; McConville et al. 1990*a*, 1990*b*; Sanal et al. 1990).

Conventional three-point location scores were calculated in order to determine the most likely location of the AT locus within the candidate region surrounding and including the STMY–S144 segment described by Sanal et al. (1990). Table 6 summarizes these results for the marker pairs S84/STMY, STMY/S132, S132/DRD2, and DRD2/S144, when the recombination fraction estimates shown in figure 1 are used. The most likely location of the AT gene was within the STMY–S132 segment, telomeric to the S84–STMY segment, and centromeric to the DRD2–S144 segment. Location scores for AT at S132 and DRD2 seemed to rule out the order S132–AT–DRD2 but failed to differentiate between placing AT telomeric or centromeric to the S132–DRD2 segment. Altogether these three-point calculations presented rea-

**Table 5**

**Lod Scores for AT versus Markers in TYR–S83 Region**

| Marker/Enzyme | Lod Score at Recombination Fragment of | | | | | | Maximum Lod Score | Maximum-Likelihood Estimate of Recombination Fraction (standard error) |
|---|---|---|---|---|---|---|---|---|
| | $10^{-6}$ | .05 | .10 | .20 | .30 | .40 | | |
| TYR/*TaqI* | −47.00 | .01 | 3.40 | 4.33 | 3.08 | 1.41 | 4.43 | .17 (.04) |
| S84/*TaqI* | −33.48 | .15 | 2.36 | 2.85 | 1.89 | .72 | 2.96 | .16 (.05) |
| S385/*MspI* | −14.13 | 2.10 | 2.75 | 2.31 | 1.37 | .52 | 2.77 | .11 (.05) |
| STMY/*TaqI* | −15.46 | 14.96 | 15.28 | 11.94 | 7.38 | 3.12 | 15.47 | .08 (.02) |
| S132/*EcoRI* | −29.06 | 7.26 | 8.80 | 7.10 | 4.00 | 1.27 | 8.81 | .11 (.03) |
| DRD2/*TaqI* | −9.10 | 8.30 | 8.21 | 6.30 | 3.92 | 1.70 | 8.42 | .07 (.03) |
| S351/*MspI* | −18.35 | 13.13 | 13.13 | 9.39 | 5.08 | 1.66 | 13.48 | .07 (.02) |
| S144/*MspI* | −32.70 | 10.06 | 11.40 | 9.30 | 5.66 | 2.20 | 11.40 | .10 (.02) |
| APO/*MspI* | −16.62 | 1.93 | 3.36 | 3.35 | 2.23 | 1.01 | 3.61 | .14 (.05) |
| S29/*TaqI* | −26.68 | .15 | 2.13 | 2.69 | 1.96 | .93 | 2.74 | .17 (.05) |
| CD3G/*MspI* | −28.51 | 4.78 | 6.53 | 6.01 | 4.05 | 1.86 | 6.69 | .13 (.03) |
| CD3D/*MspI* | −4.22 | 1.10 | 1.28 | 1.08 | .69 | .30 | 1.29 | .11 (.08) |
| CD3E/*TaqI* | −25.64 | 2.19 | 4.11 | 4.24 | 2.95 | 1.36 | 4.49 | .15 (.04) |
| PBGD/*MspI* | −63.91 | −3.82 | .86 | 3.15 | 2.58 | 1.22 | 3.17 | .21 (.05) |
| THY1/*MspI* | −33.04 | 3.44 | 5.57 | 5.20 | 3.29 | 1.30 | 5.81 | .13 (.03) |
| S147/*MspI* | −8.58 | 3.26 | 3.54 | 2.77 | 1.66 | .67 | 3.55 | .09 (.04) |
| S133/*EcoRI* | −6.70 | −.51 | .02 | .29 | .25 | .13 | .29 | .23 (.15) |
| ETS1/*XbaI* | −4.61 | .30 | .74 | .98 | .85 | .51 | .98 | .20 (.12) |
| S83/*MspI* | −67.49 | −10.80 | −5.93 | −2.01 | −.52 | −.01 | .04 | .45 (.11) |

**Table 6**

**Odds for Position of AT Locus within Four Contiguous Intervals from S84 to S144, Based on Traditional Three-Point Location Scores**

| Proposed Location of AT | Odds vs. Best-supported Order |
|---|---|
| S84–STMY: | |
| AT–S84–STMY | $1:2.3 \times 10^5$ |
| S84–AT–STMY | 1:8.9 |
| **S84–STMY–AT**[a] | 1:1 |
| STMY–S132: | |
| AT–STMY–S132 | $1:7.4 \times 10^2$ |
| **STMY–AT–S132**[a] | 1:1 |
| STMY–S132–AT | $1:1.3 \times 10^8$ |
| S132–DRD2: | |
| AT–S132–DRD2 | 1:2.3 |
| S132–AT–DRD2 | $1:3.7 \times 10^3$ |
| **S132–DRD2–AT**[a] | 1:1 |
| DRD2–S144: | |
| **AT–DRD2–S144**[a] | 1:1 |
| DRD2–AT–S144 | $1:3.2 \times 10^2$ |
| DRD2–S144–AT | $1:2.8 \times 10^2$ |

[a] Best-supported order for AT, for each three-point location.

sonably convincing evidence that AT lies between STMY and S132; the odds against the next most likely order, AT–STMY–S132, were 740:1.

In an accompanying paper by Lange and Sobel (1991), a new technique is described that makes more efficient use of our marker data than do the conventional three-point location scores reported above and helps to further resolve the location of the AT gene. Through the use of Monte Carlo simulations, an approximate location score curve can be generated. These simulations sample only a limited number of marker genotype vectors for each pedigree. In fact, we sampled only about 100 marker genotype vectors per pedigree. (In the language of the Lange and Sobel [1991] paper, the number of replicates was 100, and the sampling period was 50,000). The resulting location score curve is quite striking (fig. 2). Note that log-base-10 units are used for the vertical axis of figure 2. If the peaks for the various intervals are compared, the most likely interval for the AT gene is still within the 8.1-cM segment defined by STMY and S132, the maximum location score being midway between these loci, or approximately 4 cM telomeric to STMY. The next most likely interval—i.e., within the S84–STMY segment—is more than $10^8$ times less likely than the best-supported interval. Recalculation of these curves by a second sample of 100 replicates per pedigree gave virtually identical conclusions. The substantial computation time of about 1–2 d for each sample precludes establishing upper and lower statistical envelopes for the curve in figure 2.

A support interval for the most likely location of the AT gene can be defined by first dropping a certain defined distance below the maximum location score (fig. 3) and then finding the two intersection points of the corresponding horizontal line and the location score curve (Edwards 1972; Lange and Sobel 1991). Because the magnitude of our errors in approximating the location scores is unknown, it is prudent to be conservative. For instance, if we drop 3 log-base-10 lod units below the maximum, we can identify a support interval of either 5.2 cM, sex averaged, or 2.8 cM, male specific, centered midway between STMY and S132.

## Discussion

The map presented in figure 1 contains two pairs of loci, STMY /S385 and S351/S144, that could not be placed in a definitive order by linkage analyses because of the absence of recombination between the members of each pair. PFGE is a technique that can be used to approximate the physical distance between nearby markers. "Rare cutter" restriction enzymes generate large pieces of DNA, i.e., 50–2,000 kb. If probes for the two markers in question hybridize to common

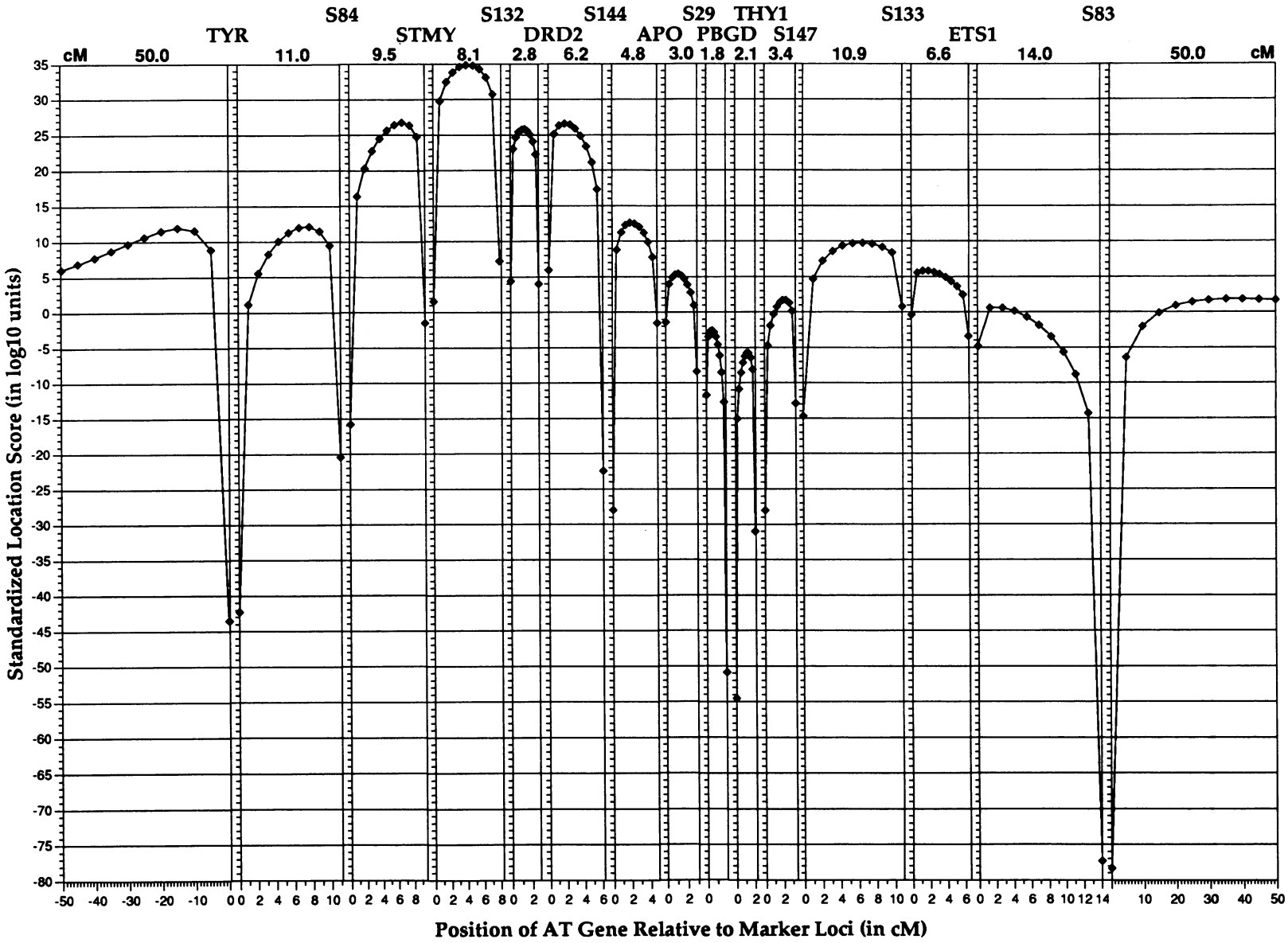


**Figure 2** Standardized location scores for 14-point map calculated by Monte Carlo simulation, using distances shown (for further details, see Lange and Sobel 1991)

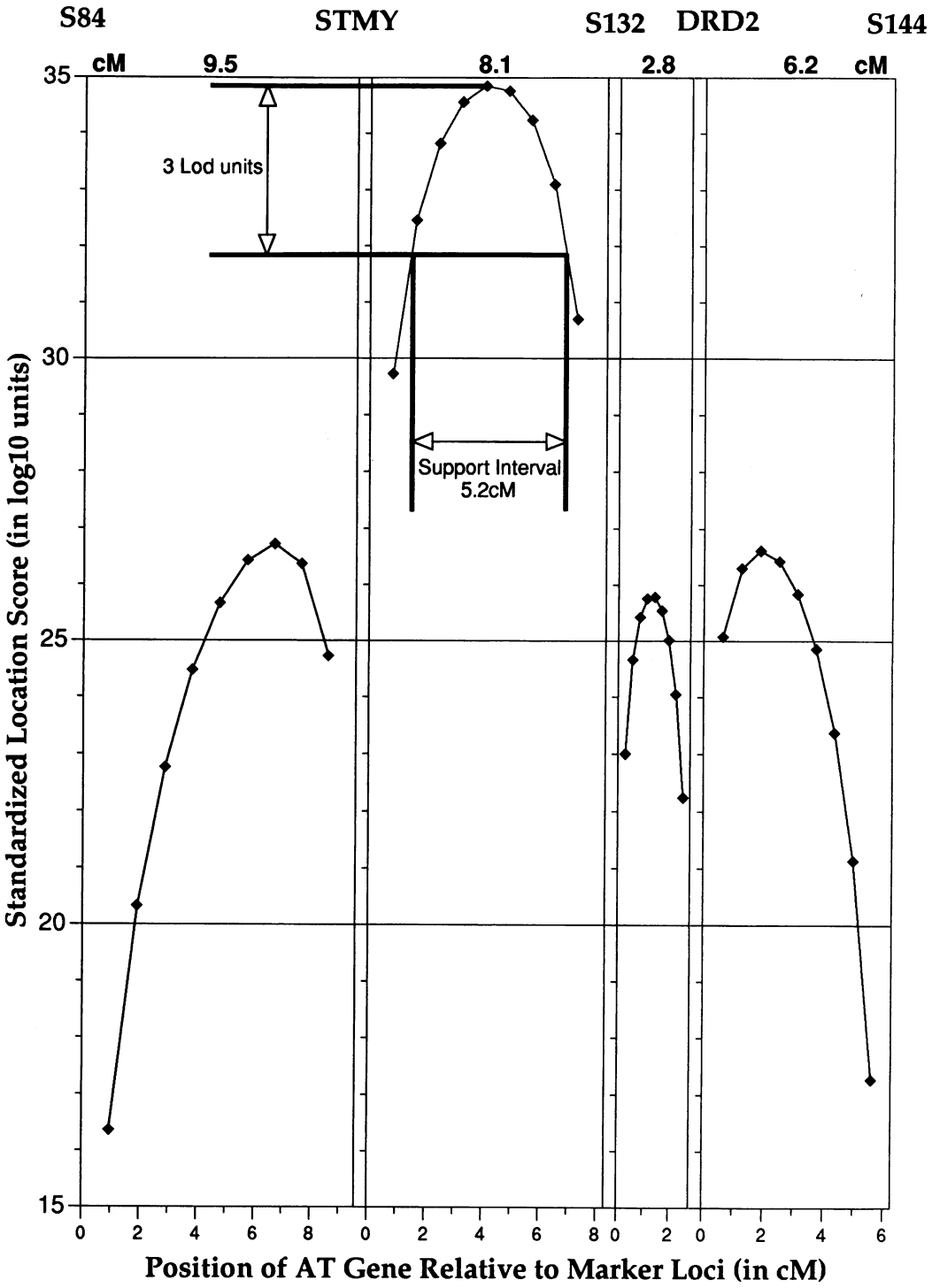


**Figure 3** Support interval, sex-averaged, for AT locus (see text for details)

PFGE-generated DNA fragments, then the distance between those markers cannot exceed the size of the smallest common DNA fragment. In this way, the pairs STMY/S385 and S351/S144 were found to reside within 60 kb and 150 kb of one another, respectively.

Our map has seven loci in common with the map of Julier et al. (1990) and is compatible with the order and approximate distances of those maps. Our ordering is also compatible with a map of structural genes in the 11q22–23 region (Charmley et al. 1991).

The 17-cM distance between STMY and S144, shown in figure 1, updates our previous estimate of 31 cM (Charmley et al. 1990*a*). This revision is based both on the characterization of more individuals and on a greater saturation of markers in the region. An accurate assessment of distance in this region is essential to the ultimate isolation of the AT gene(s).

It was surprising—and somewhat disappointing—that linkage analysis of seven RFLPs in a 17-cM region between STMY and S144 revealed three tight clusters of loci, rather than a more evenly dispersed, higher-resolution map. No recombinants were seen either between S35, STMY, and S385; between NCAM and DRD2; or between S351 and S144 (fig. 1; Julier et al. 1990; McConville et al. 1990*a;* Charmley et al. 1991; authors' unpublished data). PFGE has confirmed the close proximity of these clustered loci (table 4; also see McConville et al. 1990*a*). Our selection of restriction enzymes yielding smaller fragments than those reported by McConville et al. (1990*a*) allowed us to further reduce the distance between STMY and S385 (i.e., from 400 kb to 60 kb) and between S351 and S144 (i.e., from 560 kb to 150 kb). On the other hand, whereas McConville et al. (1990*a*) observed common-sized fragments between DRD2 and NCAM (the smallest being an *Xma*III 500-kb fragment), our experiments with different enzymes failed to identify common fragments between these probes.

We observed common fragments between S132 and NCAM, with two enzymes, the smallest fragment placing the two markers within 340 kb of one another. Thus, our localization of the AT gene(s) between STMY and S132 may be equivalent to the localization by McConville et al. (1990*a*), placing the AT gene(s) between STMY and NCAM. The AT consortium studies of NCAM polymorphisms and the precise localization of NCAM by linkage analysis within the CEPH families are still in progress.

Genetic heterogeneity was expected to be a major obstacle to linkage analyses of AT. Five complementation groups had been described (A, C, D, E, and V1) (Jaspers et al. 1988). Groups A, C, D, and E are clinically indistinguishable from one another. However, our initial data linking AT (group A) to 11q22–23 also showed that families unassigned to a complementation group increased rather than decreased lod scores, suggesting homogeneity, or clustering of genes. More recently, we have shown that group C also links to the same 11q23 markers as do the Group A families (Ziv et al. 1991). Further, Ejima et al. (1990) and Komatsu et al. (1990) have corrected the radiosensitivity of group D fibroblasts by fusion with a hybrid containing a normal human chromosome 11q. Together, groups A, C, and D constitute 97% of all tested AT families (Jaspers et al. 1988). For these reasons, we have elected to postpone further analyses of heterogeneity until most recombination events in the AT families can be delimited by closely flanking markers. The international scope of the AT consortium families should provide a stringent test of the heterogeneity issue. Meanwhile, all putative recombinants in our data base have been rechecked and are accurate. We find no appreciable double recombinants between STMY and S132.

The Monte Carlo simulation technique applied to the AT consortium data has allowed us to localize the AT gene to within an 8-cM sex-averaged interval defined by STMY and S132, with a conservative sex-averaged support interval of 5.2 cM. Using the interval-specific sex-difference distance ratio (female:male) of 2.72:1 (based on the work of Charmley et al. [1990]) delimits the male-specific support interval containing the AT gene(s) to 2.8 cM. This confirms and further refines the previous localizations by Gatti et al. (1988*a,* 1990), Sanal et al. (1990), and McConville et al. (1990*a,* 1990*b*). However, none of these previous reports considers the possibly closest flanking marker, S132. The power of the new location score method is well illustrated on the complex inbred pedigrees of the current AT consortium. The improvement in odds for the 14-point location scores (fig. 2) versus the exact three-point location scores (table 6) is encouraging for studies aimed at further localizing the AT gene(s).

## Acknowledgments

We wish to thank M. Fiorilli, L. Businco, C. Borrone, E. Galli, V. Monafo, and F. Aiuti for referring families for

this study. This work was supported by grants from the U.S. Department of Energy (to R.A.G.), American Cancer Society (to P.Co), Cancer Research Campaign, U.K. (A.M.R.T.), Italian CNR Oncology Project (L.C.), Ataxia-Telangiectasia Medical Research Foundation, and NATO Visiting Scientist (A.T.); by an NIH Biomathematics training grant (T.F.); and by NIH Genetics training grant (P.Ch.). K.L. and R.A.G. are members of the Jonsson Comprehensive Cancer Center and received core support from a USPHS grant.

## References

Boder E (1985) Ataxia-telangiectasia: an overview. In: Gatti R, Swift M (eds) Ataxia-telangiectasia: genetics, neuropathology, and immunology of a degenerative disease of childhood. Alan R Liss, New York pp 1–63

Budarf M, Sellinger B, Griffin C, Emmanuel BS (1989) Comparative mapping of the constitutional and tumor-associated 11;22 translocations. Am J Hum Genet 45: 128–139

Carlson M, Nakamura Y, Krapcho K, Payson R, O'Connell P, Leppert M, Lathrop GM, et al (1988) Isolation and mapping of a polymorphic DNA sequence MCT128.1 on chromosome 11 (D11S2185). Nucleic Acids Res 16:378

Charmley P, Foroud T, Wei S, Concannon P, Weeks D, Lange K, Gatti RA (1990*a*) A primary linkage map of the human chromosome 11q22–23 region. Genomics 6:316–323

Charmley P, Nguyen J, Tedder TF, Gatti RA (1990*b*) A frequent human CD20 (B1) differentiation antigen DNA polymorphism detected with MspI is located near 11q12–13. Nucleic Acids Res 18:207

Charmley C, Nguyen J, Wei S, Gatti RA (1991) Genetic linkage analysis and homology of syntenic relationships of genes located on human chromosome 11q. Genomics 10:606–617

Charmley P, Sanal O, Wei S, Chao A, Terhorst C, Gatti RA (1989*a*) Human T-cell receptor CD3-epsilon (CD3E)/TaqI DNA polymorphism. Nucleic Acids Res 176:2374

Charmley P, Wei S, Sanal O, Malhotra U, Concannon P, Terhorst C, Gatti RA (1989*b*) Human T-cell receptor CD3-gamma (CD3G)/MspI DNA polymorphism. Nucleic Acids Res 17:2373

Concannon P, Malhotra U, Charmley P, Reynolds J, Lange K, Gatti RA (1990) The ataxia-telangiectasia gene (ATA) on chromosome 11 is distinct from the ETS-1 gene. Genomics 46:789–794

Curry CJR, Tsai J, Hutchinson HT, Jaspers NGJ, Wara D, Gatti RA (1989) $AT_{Fresno}$: a phenotype linking ataxia-telangiectasia with the Nijmegen breakage syndrome. Am J Hum Genet 45:270–275

Dausset J (1986) Le Centre d'Etude du Polymorphisme Humain. Presse Med 15:1801–1802

Dausset J, Cann H, Cohen D, Lathrop M, Lalouel JM, White R (1990) Centre d'Etude du Polymorphisme Humain (CEPH): collaborative gene mapping of the human genome. Genomics 6:575–577

Dickson G, Gower HJ, Barton H, Prentice HM, Elsom VL, Moore SE, Cox RD, et al (1987) Human muscle neural cell adhesion molecule (N-CAM): identification of a muscle-specific sequence in the extracellular domain. Cell 50:1119–1130

Donis-Keller H, Green P, Helms C, Cartinhour S, Weiffenbach B, Stephens K, Keith TP, et al (1987) A genetic linkage map of the human genome. Cell 51:319–337

Edwards AWF (1972) Likelihood. Cambridge University Press, Cambridge

Ejima Y, Oshimura M, Sasaki MS (1990) Establishment of a novel immortalized cell line from ataxia telangiectasia fibroblasts and its use for the chromosomal assignment of radiosensitivity gene. Int J Radiat Biol 58:989–997

Gatti RA, Berkel I, Boder E, Braedt G, Charmley P, Concannon P, Ersoy F, et al (1988*a*) Localization of an ataxia-telangiectasia gene to chromosome 11q22–23. Nature 336:577–580

Gatti RA, Chessa L, McConville C, Sanal O, Ziv Y, Wei S, Tolun A, et al (1990) Chromosome 11 contains genes for the three most common complementation groups of ataxia-telangiectasia: a consortium report. Am J Hum Genet 47 [Suppl]: A179

Gatti RA, Concannon P, Salser W (1984) Multiple use of Southern blots. BioTechniques 2:148–155

Gatti RA, Lathrop GM, Salser W, Silver J, Lalouel JM, White R (1987) Localization of thy-1 with respect to a primary linkage map of chromosome 11q. Cytogenet Cell Genet 46:618

Gatti RA, Shaked R, Wei S, Koyama M, Salser W, Silver J (1988*b*) DNA polymorphism in the human thy-1 gene. Hum Immunol 22:145–150

Gold DP, Puck JM, Pettey CL, Cho M, Colligan J, Woody JN, Terhorst C (1986) Isolation of cDNA clones encoding the 20 kD nonglycosylated polypeptide chain (T3-epsilon) of the human T cell receptor/T3 complex. Nature 321: 431–434

Goridis C, Hirn M, Santoni MJ, Gennarini G, Deagostini-Bazin H, Jordan BR, Kiefer M, et al (1985) Isolation of mouse N-CAM related cDNA: detection and cloning using monoclonal antibodies. EMBO J 4:631–635

Grandy DK, Litt M, Allen L, Bunzow JR, Marchionni M, Makam H, Reed L, et al (1989) The human dopamine $D_2$ receptor gene is located on chromosome 11 at q22-q23 and identifies a *Taq*I RFLP. Am J Hum Genet 45:778–785

Jaspers NGJ, Gatti RA, Baan C, Linssen PCML, Bootsma D (1988) Genetic complementation analysis of ataxia-telangiectasia and Nijmegen breakage syndrome: a survey of 50 patients. Cytogenet Cell Genet 49:259–263

Jaspers NGJ, Painter RB, Paterson MC, Kidson C, Inoue T (1985) Complementation analysis of ataxia-telangiectasia. In: Gatti RA, Swift M (eds) Ataxia-telangiectasia: genetics, neuropathology, and immunology of a degenerative disease of childhood. Alan R Liss, New York pp 147–162

Julier C, Nakamura Y, Lathrop M, Lalouel J-M, White R (1989) Isolation and mapping of a polymorphic DNA sequence (HBI18P1) on chromosome 11 (D11S147). Nucleic Acids Res 17:9510

Julier C, Nakamura Y, Lathrop M, O'Connell P, Leppert M, Litt M, Mohandas T, et al (1990) Detailed map of the long arm of chromosome 11. Genomics 7:335–345

Kerckaert JP, Dozier C, Loucheux-Lefebvre MH, Stehelin D (1987) SstI RFLP linked to the human *ets-1* gene. Nucleic Acids Res 15:5905

Komatsu K, Kodama S, Okumura Y, Koi M, Oshimura M (1990) Restoration of radiation resistance in ataxia telangiectasia cells by the introduction of normal human chromosome 11. Mutat Res 235:59–63

Krissansen GW, Owen MJ, Verbi W, Crumpton MJ (1986) Primary structure of the T3 gamma subunit of the T3/T cell antigen receptor complex deduced from cDNA sequences: evolution of the T3 gamma and delta subunits. EMBO J 5:1799–1800

Kwon BS, Haq AK, Pomerantz SH, Halaban R (1987) Isolation and sequence of a cDNA clone for human tyrosinase that maps at the mouse c-albini locus. Proc Natl Acad Sci USA 84:7473–7477

Lange K, Goradia TM (1987) An algorithm for automatic genotype elimination. Am J Hum Genet 40:250–256

Lange K, Sobel E (1991) A random-walk method for computing genetic location scores. Am J Hum Genet 49:1320–1334

Lange K, Weeks DE (1989) Efficient computation of lod scores: genotypic elimination, genotypic redefinition, and hybrid maximum likelihood algorithms. Ann Hum Genet 53:67–83

Lange K, Weeks DE, Boehnke M (1988) Programs for pedigree ananysis: MENDEL, FISHER, and dGENE. Genet Epidemiol 5:471–472

Leppert M, O'Connell P, Nakamura Y, Lathrop GM, Maslen C, Litt M, Cartwright P, et al (1987) A partial primary genetic linkage map of chromosome 11. Cytogenet Cell Genet 46:648

Lichter P, Tang C-JC, Call K, Hermanson G, Evans GA, Housman D, Ward D (1990) High-resolution mapping of human chromosome 11 by in situ hybridization with cosmid clones. Science 247:64–69

Llewellyn DH, Kalsheker NA, Elder GH, Harrison PR, Chretien S, Goosens M (1987) A MspI polymorphism for the human porphobilinogen deaminase gene. Nucleic Acids Res 15:1349

McConville CM, Formstone CJ, Hernandez D, Thick J, Taylor AMR (1990*a*) Fine mapping of the chromosome 11q22–23 region using PFGE, linkage and haplotype analysis: localization of the gene for ataxia telangiectasia to a 5 cM region flanked by NCAM/DRD2 and STMY/S385, ph2.22. Nucleic Acids Res 18:4335–4343

McConville C, Woods CG, Farrall M, Metcalfe JA, Taylor AMR (1990*b*) Analysis of 7 polymorphic markers at chromosome 11q22–23 in 35 ataxia telangiectasia families: further evidence of linkage. Hum Genet 85:215–220

Malhotra U, Concannon P (1989) Human T-cell receptor CD3-delta (CD3D)/MspI DNA polymorphism. Nucleic Acids Res 17:2373

Maslen CL, Jones C, Glaser T, Magenis RE, Sheehy R, Kellogg J, Litt M (1988) Seven polymorphic loci mapping to human chromosomal region 11q22-qter. Genomics 2:66–75

Mietus-Snyder M, Charmley P, Korf B, Ladies JAA, Gatti RA, Karathanasis SK (1990) Genetic linkage of the human apolipoprotein AI-CIII-AIV gene cluster and the neural cell adhesion molecule (NCAM) gene. Genomics 7:633–637

Nakamura Y, Leppert M, O'Connell P, Wolff R, Holm T, Culver M, Martin DC, et al (1987) Variable number of tandem repeat (VNTR) markers for human gene mapping. Science 235:1616–1622

Reed KC, Mann DA (1985) Rapid transfer of DNA from agarose gels to nylon membranes. Nucleic Acids Res 13:7207–7221

Sacchi N, Watson DK, Guerts van Kessel AHM, Hagemeijer A, Kersey J, Drabkin HD, Patterson D, et al (1986) Hu-ets-1 and Hu-ets-2 genes are transposed in acute leukemias with (4;11) and (8;21) translocations. Science 231:379–382

Sanal O, Wei S, Foroud T, Malhotra U, Concannon P, Charmley P, Salser W, et al (1990) Further mapping of an ataxia-telangiectasia locus to the chromosome 11q23 region. Am J Hum Genet 47:860–866

Spritz R, Strunk K, Oetting W, King R (1988) RFLP for TaqI at the human tryosinase locus. Nucleic Acids Res 16:9890

Spurr NK, Gough AC, Gosden J, Rout D, Porteous DJ, van Heyningen V, Docherty AJ (1988) Restriction fragment length polymorphism analysis and assignment of the metalloproteinases stromelysin and collagenase to the long arm of chromosome 11. Genomics 2:119–127

Tedder TF, Streuli M, Schlossman SF, Saito H (1988) Isolation and structure of a cDNA encoding the B1 (CD20) cell-surface antigen of human B lymphocytes. Proc Natl Acad Sci USA 85:208–212

van den Elsen P, Shepley B-A, Borst J, Colligan J, Markham AF, Orkin S, Terhorst C (1984) Isolation of cDNA clones encoding the 20K T3 glycoprotein of the human T-cell receptor complex. Nature 312:413–418

Warnich L, Kotze MJ, Retief AE, Dietzsch E, Fox MF,

Kotze GM, Nicholson DL, et al (1986) An anonymous human single copy genomic clone, D11S29 (L7) at 11q23, identifies a moderately frequent RFLP. Nucleic Acids Res 14:1920

Weeks DE, Lange K (1987) Preliminary ranking procedures for multilocus ordering. Genomics 1:236–242

Wei S, Rocchi M, Archidiacono N, Sacchi N, Romeo G, Gatti RA (1990) Physical mapping of the chromosome 11q region containing the ataxia-telangiectasia locus. Cancer Genet Cytogenet 46:1–8

Young BR, Painter RB (1989) Radioresistant DNA synthesis and human genetic diseases. Hum Genet 82:113–117

Ziv Y, Rotman G, Frydman M, Dagan J, Cohen T, Foroud T, Gatti RA, et al (1991) The ATC (ataxia-telangiectasia group C) locus localizes to chromosome 11q22-q23. Genomics 9:373–375